Alteration of Heme Axial Ligands in Hemoglobin by Organic Solvents Analyzed by CD, FTIR, and XANES Techniques†

Christian Zentz,‡ Said El Antri,‡ Serge Pin,‡ Robert Cortes,§ Alain Massat,∥ Monique Simon,∥ and Bernard Alpert*,‡

Laboratoire de Biologie Physico-Chimique, Université de Paris VII, 2 place Jussieu, 75251 Paris Cedex 05, France, Laboratoire de Physique des Liquides et Electrochimie, CNRS LP 15, associé à l'Université Pierre et Marie Curie, 75231 Paris Cedex 05, France, LURE (CNRS LP 8, CEA, MEN) Université Paris Sud, Bâtiment 209, 91405 Orsay Cedex, France, and I.T.O.D.Y.S., Université de Paris VII, 1 rue Guy De La Brosse, 75007 Paris, France

Received June 27, 1990; Revised Manuscript Received October 11, 1990

ABSTRACT: The effects of mixed solvents on the ligand binding site in hemoglobin have been investigated though three spectroscopic techniques. Two classes of organic solvents (amides and alcohols) known to increase or decrease the hemoglobin affinity have been choosen for this study. The analysis of the iron CO stretching band shows that the ligand binding sites of αCO and βCO subunits inside the $\alpha_2\beta_2$ hemoglobin tetramer exhibit multiple conformations. From the circular dichroism and X-ray absorption near-edge structure data, it appears that no core deformation or heme reorientation occur with the affinity changes. The iron–ligand average bond angle is the sole parameter that depends on the external solvent. Since cosolvents seem to affect the dynamics rather than the hindrance of the heme cavity, we suggest that the protein affinity could be associated with a hierarchy of subtle dynamic states.

It is well-known that the affinity of hemoglobin for oxygen is markedly influenced by the presence of particular organic solvents (alcohols and amides) in the assay medium (Cordonne et al., 1979, 1981). These solvents do not act through a specific protein binding site (Dreyfus et al., 1984). The observed changes in oxygen affinity are thought to result from protein constraints, inducing porphyrin macrocycle changes (Perutz, 1970) or small distortions in the iron–oxygen bond (Shaanan, 1982, 1983). Both of the latter effects have been largely investigated on crystallized heme proteins by X-ray diffraction (Huber et al., 1970; Padlan & Lowe, 1975; Heidner et al., 1976; Phillips, 1978, 1980; Baldwin, 1980; Kuriyan et al., 1986) and neutron diffraction (Norvell et al., 1975; Phillips & Schoenborn, 1981). However, heme protein molecules in solution do not have the rigidity that they exhibit in the crystal form (Makinen et al., 1979; Kawamura-Konishi & Suzuki, 1988; El Antri et al., 1989a). Spectroscopic techniques such as circular dichroism (Sugita et al., 1971; El Antri et al., 1989b), infrared absorption of CO stretching vibration (Makinen et al., 1979; Choc & Caughey, 1981) or X-ray absorption near-edge structure (XANES) of the iron (Durham et al., 1983; Pin et al., 1985; Bianconi et al., 1986; Amiconi et al., 1989) provide information on the structural and dynamic properties of the solubilized protein. Using these three techniques we have investigated the effects of two amides and two alcohols on the possible alterations of the heme (core deformation or heme tilt) as well as the iron–ligand bonding geometry. The results on the hemoglobin molecule in organic solvent mixtures disprove the general idea of one or two fixed iron–ligand configurations as it was seen on crystalline heme proteins (Heidner et al., 1976; Baldwin, 1980; Shaanan, 1982, 1983; Kuriyan et al., 1986). Since proteins in solution are dynamic (Linderstrom-Lang, 1955; Hvidt & Nielsen, 1966; Lakowicz & Weber, 1973; Alpert & Lindqvist, 1975; McCammon et al., 1977; Frauenfelder et al., 1979, 1988; Karplus & McCammon, 1981; Somogyi et al., 1984) the present work attempts a dynamic investigation of the ligand binding site in hemoglobin and suggests that the interconvertible heme pocket conformers (Choc & Caughey, 1981) involve continuous motions of the heme axial ligand.

Materials and Methods

Preparation. Oxyhemoglobin (HbO_2) was extracted from fresh human blood and purified by standard procedures (Perutz, 1968). Hemoglobin was stripped of 2,3-diphosphoglycerate by passing the hemoglobin solution through an AG 501 Bio-Rad resin (Jelkmann & Bauer, 1976). This stripped hemoglobin was concentrated up to 20 mM in heme by vacuum filtration and, simultaneously, adjusted to pH 7.3 by dialysis against a potassium/sodium phosphate buffer. The carbon monoxide hemoglobin derivative (HbCO) was prepared from this HbO_2 solution by its exposure to 1 bar of pure carbon monoxide (CO) gas (Alben & Bare, 1980).

The effects of organic solvents were studied at a molar fraction of 3.2 mol % ethanol, 2.1 mol % propanol, 4.8 mol % formamide, or 6.1 mol % acetamide (Cordonne et al., 1981) in phosphate buffer, pH 7.3. The potassium/sodium phosphate concentrations were 50 mM for the circular dichroic experiments (protein concentration $\simeq$ 1 mM in heme) and 200 mM for XANES and infrared spectroscopy (protein from 10 to 14 mM). Each sample was centrifugated at 18000 rpm after the addition of cosolvents. Experiments on HbO_2 or HbCO, with or without cosolvent, were carried out at a temperature of 20 °C. The quality of each sample was checked by optical absorption (350–700 nm) before and just after each measurement on a Cary 219 Varian spectrophotometer.

Circular Dichroism (CD) Study. Circular dichroic studies in the Soret and visible ranges were carried out on a Jobin Yvon Mark V dichrograph with a 0.5-nm band width. The sensitivity scale was set to a dichroic absorbance of 5×10^{-6} mm^{-1} on the recorder chart. In each case the recording was

† This research was supported in part by a grant from La Fondation de France.

* To whom correspondence should be addressed.
‡ Laboratoire de Biologie Physico-Chimique, Université de Paris VII.
§ Université Pierre et Marie Curie and Université Paris Sud.
∥ I.T.O.D.Y.S., Université de Paris VII.

0006-2960/91/0430-2804$02.50/0 © 1991 American Chemical Society

Table I: Cosolvent Effect on Hemoglobin Affinity for Oxygen[a]

cosolvent	molar fractn (%)	log P_{50} (mmHg)	cooperative index
ethanol	3.2	1.39	2.74
2-propanol	2.1	1.36	2.57
formamide	4.8	0.76	2.76
acetamide	6.1	0.83	2.57

[a] Cordone et al., 1981.

repeated three to five times. The data were expressed in terms of molecular ellipticity (θ).

Fourier Transform Infrared (FTIR) Study. Infrared spectra, at 2-cm^{-1} resolution, were performed in cells with calcium fluoride windows and a 25-μm path length. Spectra were measured with a 60SX Nicolet spectrophotometer. Each spectrum results from the computerized accumulation of 900 scans between 1200 and 4000 cm^{-1}. To remove instrumental contributions to absorbance, spectra were computed by using an air reference.

The iron CO stretching band was explored between 1920 and 1980 cm^{-1}. To remove solvent and protein contributions to infrared absorbance, the different spectra of CO stretching were determined by subtraction of the HbO_2 spectrum from the HbCO spectrum collected under the same conditions (Alben & Caughey, 1968). Thus, the absorption spectrum due to the CO ligated to the iron gives a signal with negligible background contribution and a baseline closest to zero.

X-ray Absorption Near-Edge Structure (XANES) Study. X-ray absorption K-edge values of the iron have been obtained with synchrotron radiation from the DCI electron storage ring at LURE (Orsay, France). The experiments were performed on the EXAFS II set up with a Si 511 monochromator and a NaI detector (in front of which a 20-μm Mn filter was set) placed at 90° from the incident beam in the horizontal plane. X-ray absorption measurements were made by the total fluorescence emission of the iron as a function of incident X-ray energy. Under these experimental conditions, the monochromator slit allows a resolution (full width at half-maximum) of 0.8 eV. Measurements were performed on a thin-layer sample (20 × 5 mm^2), each scan being collected: with a 0.2-eV step and 5-s integration time in the 7090–7160-eV range; with a 5-eV step and 3-s integration time in the 7160–7500-eV range. Each K-edge spectrum was the average of three scans. Subtraction of the scattering background was made before normalization of the ratio of the fluorescence intensity to the incident X-ray intensity. All spectra were normalized to the iron atomic absorption obtained by linear fitting of the EXAFS oscillations in the 7160–7500-eV range (Bianconi et al., 1984). The zero of the energy scale (E_0) for each liganded hemoglobin form (HbCO or HbO_2) has been chosen at the iron absorption situated at the first maximum of the XANES-derived spectrum (Bianconi et al., 1984).

Results

Circular Dichroic Study of the Heme. Under our experimental conditions, the cosolvents increase (amides) or decrease (alcohols) the affinity (P_{50}) of the hemoglobin molecule for oxygen (see Table I) (Cordonne et al., 1981). Since these P_{50} variations are thought to be related to local distortions in the heme region (Perutz, 1970), circular dichroic (CD) spectra of the Soret and visible wavelength domains of the heme were collected.

In the Soret region, the CD spectra of the oxyhemoglobin in the presence of the cosolvents (data not shown) do not exhibit a different pattern relative to the protein in standard

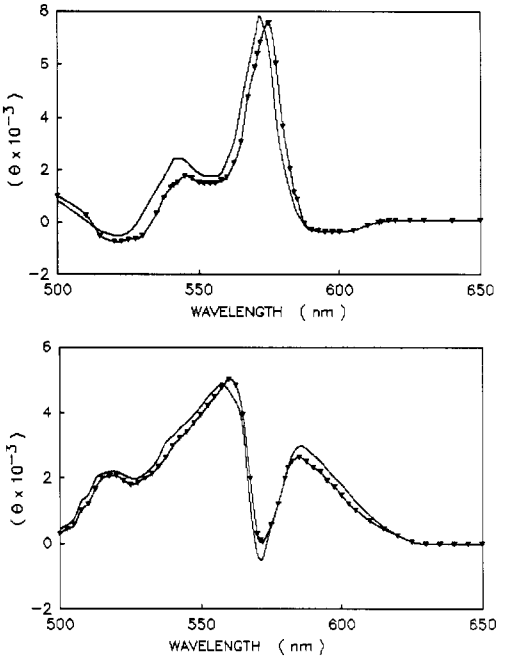

FIGURE 1: Circular dichroic spectra of liganded hemoglobin in the visible domain. The CD data are expressed in terms of molecular ellipticity θ (deg cm^2 $dmol^{-1}$) on a heme basis. Top: oxyhemoglobin (—) without and (▽) with 6.1 mol % acetamide. Bottom: carboxyhemoglobin (—) without and (▽) with 6.1 mol % acetamide. Both spectra were measured with 1 mM (in heme) hemoglobin in 50 mM phosphate, pH 7.3.

buffer conditions (Sugita et al., 1971). Thus no apparent changes in the interactions of the heme with the apoprotein are detected. This suggests that no appreciable distortion or tilting of the heme macrocycle and hence no significant movements of the particular residues that participate in the rotational strength of the heme transitions (Hsu & Woody, 1971) are produced by these organic solvents.

In contrast, the cosolvents produce small shifts in the visible domain of the CD spectra. The spectra of HbCO and HbO_2 with and without acetamide are shown, for example, in Figure 1. Superimposed on the rotational strength of the heme transitions, the iron–ligand geometry influences the CD visible spectrum (Garnier et al., 1972). Eaton's attribution (Eaton & Hofrichter, 1981, and references cited therein) suggest that the negative band V (545 nm) of the iron–ligand transition is involved in the HbO_2 CD spectrum; the negative band I (658 nm) and the positive band II (560 nm) of the iron transition are implicated in the HbCO CD modification. Indeed it is known that the Fe d_π electrons compete between the CO and porphyrin π^* orbitals (Zerner et al., 1966). Fe–CO bending or tilting misaligns the Fe and porphyrin π orbitals and induces Fe→porphyrin or Fe→CO back-bonding variations in opposite directions (Satterlee et al., 1978; Li & Spiro, 1988).

To ascertain that only the iron–ligand geometry is altered by the cosolvents, it was interesting to consider the CD visible spectrum of the ligand-free hemoglobin (deoxy form). The absence of any cosolvent effect in the CD visible spectrum (see the case of acetamide in Figure 2) reinforces the idea that the heme organization is not affected (electronic distribution within the heme or distortion of the porphyrin core). Second, it demonstrates that each cosolvent induces constraints that favor and stabilize particular iron–ligand configurations.

Infrared Study of CO Bound to Hemoglobin. The vibration of the dioxygen bound to the heme iron presents a very low infrared band. In contrast, infrared spectra of the CO stretching frequencies can be easily used to monitor changes

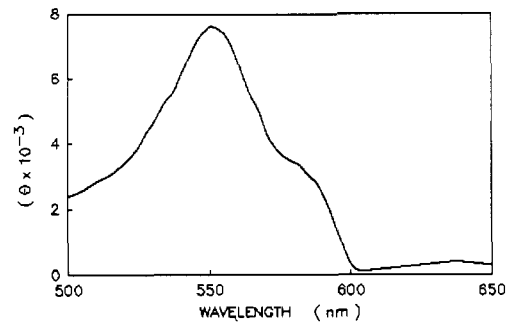

FIGURE 2: Superposition of the circular dichroic spectra in the visible domain of deoxyhemoglobin without and with cosolvent. Experimental conditions: 1 mM (in heme) hemoglobin, 50 mM phosphate, pH 7.3, ± 6.1 mol % acetamide.

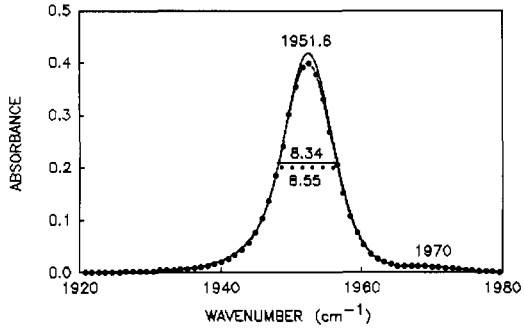

FIGURE 3: Infrared difference spectra (HbCO − HbO_2) in the CO stretch frequency region. CO stretch frequencies (—) obtained in the presence of 3.2 mol % ethanol (the band width a half-absorbancy $\Delta\sigma_{1/2}$ is 8.34 cm^{-1}) and (O) obtained in the presence of 4.8 mol % formamide ($\Delta\sigma_{1/2}$ is 8.55 cm^{-1}). Both spectra were measured with 10 mM (in heme) hemoglobin in 200 mM phosphate, pH 7.3

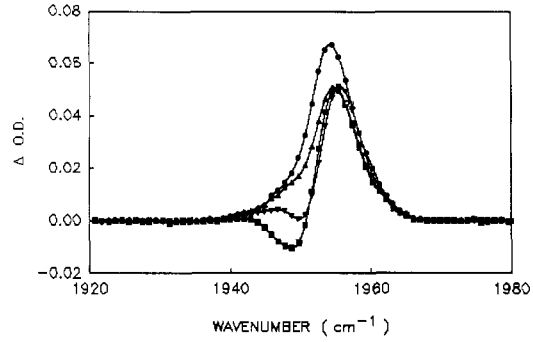

FIGURE 4: Difference between the CO stretch band absorbancies of HbCO in a cosolvent relative to HbCO in 200 mM phosphate (pH 7.3): (●) ethanol, (■) 2-propanol, (▲) formamide, and (▼) acetamide.

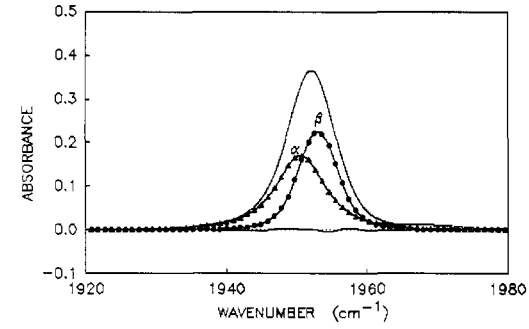

FIGURE 5: Spectra of αCO and βCO subunits inside the intact HbCO tetramer. The αCO and βCO infrared spectra were obtained according to the analyse of Urban et al. (1976). Data from 10 mM (in heme) hemoglobin and 200 mM phosphate, pH 7.3: αCO, σ_{CO} = 1950.5 cm^{-1}, $\Delta\sigma_{1/2}$ = 8.50 cm^{-1}, A = 0.172; βCO, σ_{CO} = 1953.0 cm^{-1}, $\Delta\sigma_{1/2}$ = 8.20 cm^{-1}, A = 0.225.

in the heme environment (Satterlee et al., 1978; Moffat et al., 1979). CO stretching frequencies from HbCO in the presence of cosolvents were oberved at 1951.6- and 1970-cm^{-1} wavenumbers (σ) which do not differ from CO–hemoglobin under normal conditions (Figure 3) (Alben & Caughey, 1968; Caughey et al., 1978; Choc & Caughey, 1981). The major line (1951.6 cm^{-1}) is due to the CO stretching vibration from CO bound to the iron in native hemoglobin. The very weak band at 1970 cm^{-1} is not clearly attributed (Choc & Caughey, 1981). Previous investigations on native hemoglobin have already shown that the two CO lines do not shift between pH 6 and 9 (Satterlee et al., 1978). At extreme pH values, the hemoglobin is reversibly denatured. Thus, changing the pH (from 4 to 11.9) changes the frequency slightly and produces reversible redistributions of the individual infrared band intensities (Choc & Caughey, 1981). However, the absorbancy (Satterlee et. al., 1978) and the band width at half peak height ($\Delta\sigma_{1/2}$) (Moffat et al., 1979) of the CO stretching vibration band are highly sensitive to the local environment. As seen in Figure 4, whatever the solvent, the minor band remains unaffected and the solvent-induced perturbations are only probed through alterations in the major band (1951.6 cm^{-1}). Thus, the present analysis is focused on the deviations observed in the major CO band.

The shape of this band is characterized by a parameter Pr (Massat, 1987)

$$Pr = \Delta\sigma_{1/4}/\Delta\sigma_{1/2}$$

which is the ratio between the width ($\Delta\sigma$) of the band at $^1/_4$ and $^1/_2$ of the absorbance. If the band is a pure Lorentzian the ratio is 1.73 and 1.41 for a pure Gaussian (Massat, 1987). The major CO stretching vibration band has a mixed shape as defined by Urban et al. (1976): Gaussian in the top and Lorentzian in the bottom. In the phosphate buffer, Pr is 1.499. The Lorentzian character in this mixed band increases in the presence of the alcohols (Pr = 1.503), while it decreases with the amides (Pr = 1.494).

The single band at 1951.6 cm^{-1} observed in the HbCO spectrum results from the overlapping of the αCO and βCO vibrational bands inside the $\alpha_2\beta_2$ tetramer (Satterlee et al., 1978; Potter et al., 1983). Thus, the major CO vibrational band envelope of HbCO has been approximated by the simple summation of spectra of both α and β isolated subunits (Potter et al., 1983). According to this spectral analysis, the α and β bands can be deconvoluted with one theoretical curve in solution and at least two curves in the crystal (Potter et al., 1985). Nevertheless, multiple infrared CO stretching bands have been observed in the HbCO spectrum (Caughey et al., 1978; Choc & Caughey, 1981; Brown et al., 1983). Four bands yield a satisfactory fit of the HbCO spectrum when the analysis is based on a linear combination of 30% Lorentzian and 70% Gaussian functions (Potter et al., 1990).

These different analyses all assume that the CO vibrational bands of the isolated subunits are indistinguishable from the subunits within the $\alpha_2\beta_2$ tetramer. We have thus preferred the method of deconvolution of Urban et al. (1976) using two vibrational bands that must represent the CO infrared spectra of the α and β subunits within the $\alpha_2\beta_2$ tetramer. The comparison of the results with the σ_{CO} of the α and β isolated subunits allows for the assignment of the band positions of the α and β chains inside the tetramer. For the decomposition, we have used two profile functions of second order (Urban et al., 1976). Under normal buffered conditions, we observe the σ_{CO} stretching frequencies of α and β chains at 1950.5 and 1953 cm^{-1} with a $\Delta\sigma_{1/2}$ of 8.5 and 8.2 cm^{-1}, respectively (see Figure 5). This analysis gives, for the α and β chains, σ_{CO}

Table II: Relative Area (%) of Component Bands of α and β Chains[a]

sample	α chain			β chain		
	band 1	band 2	band 3	band 1	band 2	band 3
200 mM phosphate, pH 7.3	25.8 (1949.0)	38.2 (1950.2)	36.0 (1952.1)	12.5 (1951.4)	68.0 (1952.8)	19.5 (1954.8)
+3.2 mol % ethanol	17.0 (1947.8)	57.0 (1950.7)	26.0 (1953.2)	19.4 (1951.1)	57.0 (1953.5)	23.6 (1955.8)
+2.1 mol % 2-propanol	11.6 (1948.1)	72.0 (1950.9)	16.4 (1953.8)	14.6 (1951.8)	64.6 (1953.7)	20.8 (1955.7)
+4.8 mol % formamide	21.6 (1947.5)	47.8 (1950.7)	30.6 (1953.3)	18.0 (1951.6)	56.0 (1953.6)	26.0 (1955.3)
+6.1 mol % acetamide	23.4 (1949.3)	49.0 (1950.8)	27.6 (1952.0)	18.1 (1952.4)	54.6 (1953.8)	27.3 (1955.2)

[a] The frequency center (cm^{-1}) is in parentheses.

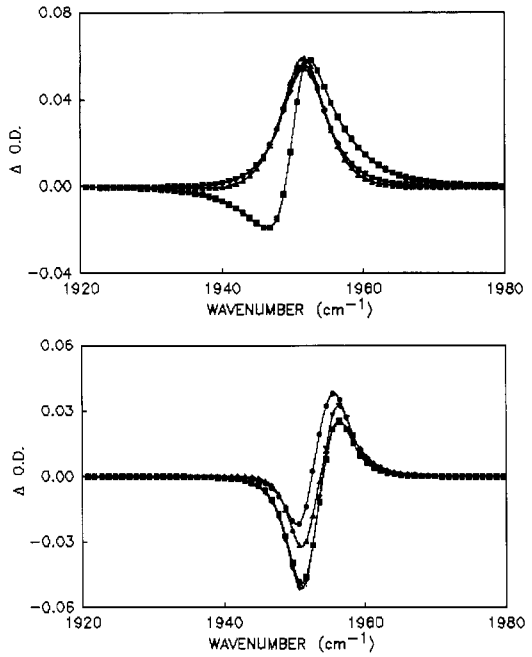

FIGURE 6: Difference spectra of αCO (top) and βCO (bottom) stretching bands of HbCO in (●) ethanol, (■) 2-propanol, (▲) formamide, and (▼) acetamide, relative to αCO and βCO, respectively, of HbCO in 200 mM phosphate buffer.

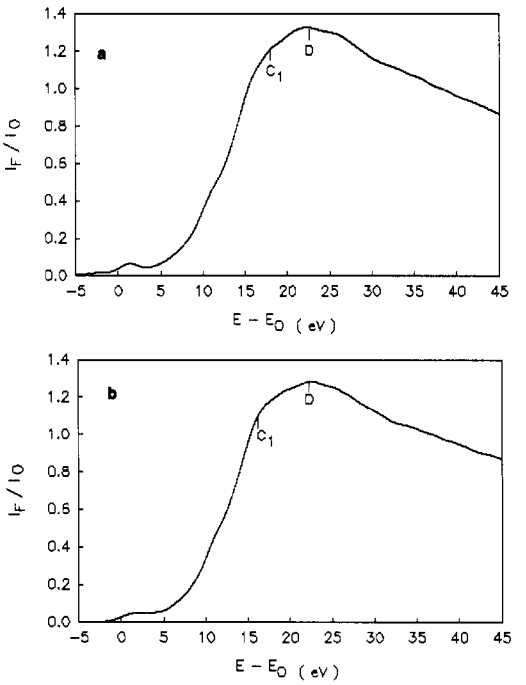

FIGURE 7: Iron XANES spectra of HbO_2 (a) and HbCO (b) in the absence of cosolvent. Experimental conditions: 14 mM (in heme) hemoglobin, 200 mM phosphate, pH 7.3. The C_1 peak intensities depend on the Fe–L bonding angle and the D peak intensities depend on the heme doming.

values slightly different from those of α and β isolated chains (Potter et al., 1983). Our results indicate that, in hemoglobin, the specificity of the apoprotein chain affects differently the iron–ligand bond. As seen from the difference infrared spectra (Figure 6) the αCO and βCO vibrational bands are sensitive to the external solvent. The CO stretching vibrations of the α and β hemes inside the hemoglobin molecule appear to be differently affected by the organic solvents.

We do not observe pure Gaussian or Lorentzian shapes for either the α or the β band. Each of these bands cannot be decomposed into less than three bands. Without cosolvents, the CO band of the α chain has a good fit with two Lorentzian bands and one mixed band with a component distribution of 25.8%, 38.2%, and 36%. The β chains have a predominant mixed component (68%) and two Lorentzian components (12.5% and 19.5%) (see Table II). This multiple-component fit appears to result from multiple protein conformers (Choc & Caughey, 1981). The prominent change induced by the cosolvent to hemoglobin points out the relative contributions of the α and β band components. And inside each α and β band, the cosolvents affect differently the relative contribution of the multiple bands. Table II displays the computed integrated relative area of the three bands modified by the cosolvents.

As previously suggested by Caughey et al. (1981) these multiple bands should reflect a dynamic aspect of the structure at the ligand binding site. The changes of the CO vibration, generated by the protein anisotropic environment, could reveal the rapidly interconverting conformers of the heme pockets. By the modulation of these dynamics, the cosolvents induce different distributions of the individual infrared CO band components. Indeed, while the absorbances of bands 1 and 3 are decreased by the cosolvents in the α chains, they are increased in the β chains. The same opposite variation of the band 2 intensities is observed when one compares α and β chains. Therefore, the heme pocket cavity as well as the carbonyl group in motion are, in the α and β chains, differently modified by the surrounding solvent.

XANES Study of Iron–Ligand and Porphyrin Configurations. XANES spectroscopy on hemoglobin in solution yields the angle Fe–L averaged on the α and β subunits (Pin et al., 1982; Congiu-Castellano et al., 1987), The XANES spectra of HbCO and HbO_2 in phosphate buffer solution are shown in Figure 7. The experimental XANES spectra exhibit C_1 and D peaks previously reported (Bianconi et al., 1985a,b; Congiu-Castellano et al., 1987). In HbCO, the C_1 and D peaks are at 16 and 22 eV, respectively (Amiconi et al., 1989). In HbO_2, the C_1 and D peaks are at 18 and 22.5 eV, respectively (Congiu-Castellano et al., 1987; Oyanagi et al., 1986). The C_1 peak is due to the multiple scattering along the z direction (normal to the heme plane); the D peak is due to multiple scattering in the porphyrin plane (x, y direction) (Bianconi et al., 1985c).

The intensity of the C_1 peak reflects the configuration of the iron–ligand angle (Cartier, 1988; Amiconi et al., 1989). The intensity of the C_1 peak of the hemoglobin under normal

Table III: Effect of Organic Cosolvents on the C_1 Peak Intensity Variations[a]

sample	ΔC_1 (±0.001) HbCO	HbO_2
R + 3.2 mol % ethanol	+0.007	+0.008
R + 2.1 mol % 2-propanol	+0.003	+0.020
R	0	0
R + 4.8 mol % formamide	−0.025	−0.021
R + 6.1 mol % acetamide	−0.010	−0.008

[a] The reference sample (R) is hemoglobin in 200 mM phosphate, pH 7.3.

buffer condition has been used as a reference (C_1^0) for the iron–ligand deviations induced by the different cosolvents. The intensity difference $\Delta C_1 = C_1 - C_1^0$ gives a direct measure of the effect of the cosolvent on the iron–ligand bonding angle deformation. This ΔC_1 allows for the calculation of the angular variation $\Delta\theta$ by comparison to the iron–ligand angle θ_0 under normal buffer condition (Amiconi et al., 1989). Table III displays the ΔC_1 values in HbCO and in HbO_2 induced by the cosolvents. From this table, it is evident that the effects of amides and alcohols on the ligand bonding angle are opposite. From Amiconi et al. (1989), the Fe–C–O and Fe–O–O configuration variations can be estimated between −4° under amides effect and +3° under alcohols effect. The absolute value of these angles must be interpreted with great caution because the data represent an average of the different iron–ligand bond angles. However, it appears that the ligand–bonding angle decreases in the order alcohols > water > amides, and, thus, the angle is higher when the affinity is lower.

Under any solvent conditions, the *D* peak intensities are 1.317 ± 0.002 for HbO_2 and 1.281 ± 0.002 for HbCO. Since, the *D* peak originates from transitions involving mainly the porphyrinic macrocycle (Morgan & Dolphin, 1987; Cartier, 1988; Amiconi et al., 1989), it is interesting to note the following.

(i) The distortion of the porphyrin macrocycle varies only slightly with the ligand nature (O_2 or CO). The heme doming variation should involve the iron–ligand bond length difference between O_2 and CO. Indeed, the chemical form of the ligand bonding should be interconnected with the structural organization of the porphyrin ring.

(ii) The *D* peak intensity does not change with changes in solvent conditions. Thus, there is a great stability of the heme doming with respect to different solution conditions. It can be reasonably hypothesized first that the size of the pocket cavity does not vary enough to perturb the overall symmetry of the heme, which remains octahedral; second, the porphyrin geometry is not altered by the presence of the cosolvents.

Therefore the average angle of the iron–ligand bond angle (see ΔC_1 variations) appears to be the sole parameter that depends on the external solvent. Thus, changes in the protein–solvent interactions perturb the protein dynamics and in this way may control the ligand-bonding properties. This could explain the apparent contradiction between the rigidity of the iron–ligand angle in crystallized hemoglobin and the multiple bonding orientations observed in hemoglobin solution (Baldwin, 1980; Shaanan, 1983; Bianconi, 1985c; Congiu-Castellano, 1987).

Discussion

In hemoglobin, the iron atom presents octahedral coordination. The ligand binds the iron (in the sixth crest) at the opposite side of the histidine F8 and exhibits, in the crystallized protein, a fixed angle with regard to the heme plane. Crystallographic studies on different heme proteins have revealed that steric restraint of the heme pocket modifies the iron–ligand configuration. For this purpose, in some heme model compounds, CO binds practically linearly and perpendicularly to the heme plane (Hoard, 1975; Peng & Ibers, 1976; Ascone et al., 1987) whereas in heme proteins the Fe–C–O linkage is distorded with respect to the heme plane (Norvell et al., 1975; Heidner et al., 1976; Baldwin, 1980; Perutz, 1989). The relation between ligand-bonding geometry and affinity was extensively investigated (Huber et al., 1970; Collman et al., 1976, 1979; Traylor & Berzinis, 1980; Traylor et al., 1981; Ward et al., 1981; Yu et al., 1983).

It is known that the alcohols (or the amides) decrease (or increase) the hemoglobin affinity for oxygen (Cordonne et al., 1981). In spite of an important affinity shift, the stereochemical characteristics of the heme macrocycle (distortion or reorientation) remain unchanged (see CD and XANES data), and only the iron ligand bond angle depends on the solvent surrounding the protein. As already stated, without significant structural distortion of the porphyrin ring, the ligand binds the iron with different orientations and can be described as resulting from different conformer populations (Choc & Caughey, 1981; Ormos et al., 1988). The multiple iron–ligand configurations cannot be calculated and the iron–ligand bond angle extracted from the XANES data in aqueous solution appears to result from an average of different orientations.

It must be noted here that our knowledge of protein structure is largely based on crystallized proteins. It is not possible to rule out the possibility that the crystal lattice induces significant strain on the hemoglobin molecule and thereby selects some particular ligand-bonding geometry that can be attributed to steric interaction of the axial ligand with surrounding amino acid residues. As a matter of example, it has been demonstrated that, below a critical temperature, the protein dynamics is no more governed by the protein medium microviscosity but rather is governed by the sole surrounding solvent (Rholam et al., 1984; Royer & Alpert, 1987). Thus, studies of macromolecules in solution, crystal, or supercooled solutions (Hori et al., 1980) do not deal with the same parameters and therefore should be compared with extreme caution.

Our observations on hemoglobin in solution show no evidence for one or two specific iron–ligand configurations. The iron–CO bond angle seems to have multiple distortions. The occupation of these different heme–CO states is extremely responsive to external influence. Since the protein fluctuates continuously, the protein motions may force the CO to large displacements that depend strongly on the external solvent. Thus, the dynamics of the heme pocket could provide different hindrances, which induce an iron–ligand conformational heterogeneity. Brown et al. (1983) have shown that the heme environment is sensitive to the hydratation level of the protein. The different solvations of the hemoglobin molecule induced by the amides, or the alcohols, could be at the origin of the dynamic modifications of the heme pockets (Singh et al., 1981). Local changes in the heme pocket can perturb the stretching vibrations of CO without affecting the heme geometry. According to the analysis of Li and Spiro (1988), the CO angular displacement in heme proteins involves iron–ligand tilting and bending as well as porphyrin buckling contributions. In solution, the continuous variation of the ligand induced by thermal agitation is perfectly described by the multiple CO-bonding geometry of the bent, linear, or tilted configurations. Conformer interconversion (Choc & Caughey, 1981) of the heme pocket would be rather continuous motions of the heme axial ligand which can be described as a distribution of the

tilt angles (Ormos et al., 1988). Solid state, or computation, converts this continuous change in discrete species to more or less tighter binding.

Within this context and according to the analysis of Li and Spiro (1988) various distortions result in an iron→ligand or an iron→porphyrin back-bonding. This back-bonding predicts the small distortions ($\leq 10°$) recently observed by X-ray diffraction (Perutz, 1989) and influences the CO vibrational pattern in relation with the heme pocket fluctuations (Satterlee et al., 1978). The two classes of cosolvents affect the dynamics rather than the hindrance of the heme cavity and do not produce the same level of disorder of the iron-ligand configurations. XANES spectroscopy yields insights into the average structure, in different solutions, of the distortion of the porphyrinic macrocycle and of the ligand-bonding geometry. The intensity of the *D* peak absorption, which is dependent upon the distortion of the whole macrocycle, shows and confirms the CD data that the cosolvents induce no or very little change in the heme geometry. The low values in the observed angular changes ($-4° \leq \Delta\theta \leq +3°$) are of the same order as those produced by the motions resulting from back-bonding under normal buffer conditions (Li & Spiro, 1988; Perutz, 1989). The small rearrangement of the iron–ligand configuration, subsequent to the solvent perturbation, demonstrates that a hierarchy of motions exists (Ansari et al., 1987) and that the protein affinity can be associated to a hierarchy of subtle conformational and dynamic states. This implies that the hemoglobin affinity variations do not result from constraints or hindrance at the heme groups but rather to different fluctuations in the heme region. Thus, the dynamic properties of the protein should be involved in the affinity changes of heme proteins.

Acknowledgments

We thank the Centre National de la Transfusion Sanguine (Paris, France) for the gift of the human red blood cells. We are very much indebted to technicians and engineers of LURE and of Linear Accelerator Laboratory (Orsay, France) for running DCI for synchrotron radiation. We thank Dr. C. Royer (University of Wisconsin, Madison) for her very helpful suggestions and her assistance with the manuscript.

Registry No. Ethanol, 64-17-5; 2-propanol, 67-63-0; formamide, 75-12-7; acetamide, 60-35-5.

References

Alben, J. O., & Caughey, W. S. (1968) *Biochemistry 7*, 175–183.

Alben, J. O., & Bare, G. H. (1980) *J. Biol. Chem. 255*, 3892–3897.

Alpert, B., & Lindqvist, L. (1975) *Science 187*, 836–837.

Amiconi, G., Santucci, R., Coletta, M., Congiu-Castellano, A., Giovannelli, A., Dell'Ariccia, M., Della Longa, S., Barteri, M., Burattini, E., & Bianconi, A. (1989) *Biochemistry 28*, 8547–8553.

Ansari, A., Berendzen, J., Braunstein, D., Cowen, B. R., Frauenfelder, H., Hong, M. K., Iben, I. E. T., Johnson, J. B., Ormos, P., Sauke, T. B., Scholl, R., Schulte, A., Steinbach, P. J., Vittitow, J., & Young, R. D. (1987) *Biophys. Chem. 26*, 337–355.

Ascone, I., Bianconi, A., Dartyge, E., Della Longa, S., Fontaine, A., & Momenteau, M. (1987) *Biochim. Biophys. Acta 915*, 168–171.

Baldwin, J. M. (1980) *J. Mol. Biol. 136*, 103–128.

Bianconi, A., Congiu-Castellano, A., Dell'Ariccia, M., Giovannelli, A., Durham, P. J., Burattini, E., & Barteri, M. (1984) *FEBS Lett. 178*, 165–170.

Bianconi, A., Congiu-Castellano, A., Dell'Ariccia, M., Giovannelli, A., Burattini, E., Castagnola, M., & Durham, P. J. (1985a) *Biochim. Biophys. Acta 831*, 120–124.

Bianconi, A., Congiu-Castellano, A., Dell'Ariccia, M., Giovannelli, A., Burattini, E., Durham, P. J., Giacometti, G. M., & Morante, S. (1985b) *Biochim. Biophys. Acta 831*, 114–119.

Bianconi, A., Congiu-Castellano, A., Durham, P. J., Hasnain, S. S., & Phillips, S. (1985c) *Nature 318*, 685–687.

Bianconi, A., Congiu-Castellano, A., Giovannelli A., Dell'-Ariccia, M.,Burattini, E., Durham, P. J., & Giacometti, G. M. (1986) *Eur. Biophys. J. 14*, 7–10.

Brown, W. E., III, Sutcliffe, J. W., & Pulsinelli, P. D. (1983) *Biochemistry 22*, 2914–2923.

Cartier, C. (1988) Ph.D. Thesis, Université Paris XI.

Caughey, W. S., Houtchens, R. A., Lanir, A., Maxwell, J. C., & Charache, S. (1978) in *Biochemical and Clinical Aspects of Hemoglobin Abnormalities* (Caughey, W. S., Ed.) pp 29–56, Academic Press, New York.

Caughey, W. S., Shimada, H., Choc, M. G., & Tucker, M. P. (1981) *Proc. Natl. Acad. Sci. U.S.A. 78*, 2903–2907.

Choc, M. G., & Caughey, W. S. (1981) *J. Biol. Chem. 256*, 1831–1838.

Collman, J. P., Brauman, J. I., Halbert, T. R., & Suslick, K. S. (1976) *Proc. Natl. Acad. Sci. U.S.A. 73*, 3333–3337.

Collman, J. P., Brauman, J. I., & Doxsee, K. M. (1979) *Proc. Natl. Acad. Sci. U.S.A. 76*, 6035–6039.

Congiu-Castellano, A., Bianconi, A., Dell'Ariccia, M., Della Longa, S., Giovannelli, A., Burattini, E., & Castagnola, M. (1987) *Biochem. Biophys. Res. Commun. 147*, 31–38.

Cordone, L., Cupane, A., San Biagio, P. L., & Vitrano, E. (1979) *Biopolymers 18*, 1975–1988.

Cordone, L., Cupane, A., San Biagio, P. L. & Vitrano, E. (1981) *Biopolymers 20*, 39–51.

Dreyfus, M., Fries, J., Tauc, P., & Hervé, G. (1984) *Biochemistry 23*, 4852–4859.

Durham, P., Bianconi, A., Congiu-Castellano, A., Giovannelli, A., Hasnain, S. S., Incoccia, L., Morante, S., & Pendry, J. B. (1983) *EMBO J. 2*, 1441–1443.

Eaton, W. A., & Hofrichter J. (1981) *Methods Enzymol. 76*, 175–261.

El Antri, S., Sire, O., & Alpert, B. (1989a) *Chem. Phys. Lett. 161*, 47–49.

El Antri, S., Zentz, C., & Alpert, B. (1989b) *Eur. J. Biochem. 179*, 165–168.

Frauenfelder, H., Petsko, G. A., & Tsernoglou, D. (1979) *Nature 280*, 558–563.

Frauenfelder, H., Parak, F., & Young, R. D. (1988) *Annu. Rev. Biophys. Chem. 17*, 451–479.

Garnier, A., Bolard, J., & Danon, J. (1972) *Chem. Phys. Lett 15*, 141–143.

Heidner, E. J., Ladner, R. C., & Perutz, M. F. (1976) *J. Mol. Biol. 104*, 707–722.

Hoard, J. L. (1975) in *Porphyrins and Metalloporphyrins* (Smith, K. M., Ed.) pp 356–358, Elsevier, Amsterdam.

Hori, H., Ikeda-Saido, M., & Yonetani, T. (1980) *Nature 288*, 501–502.

Hsu, M. C., & Woody, R. W. (1971) *J. Am. Chem. Soc. 93*, 3515–3525.

Huber, R., Epp, O., & Formanek, H. (1970) *J. Mol. Biol. 52*, 349–354.

Hvidt, A., & Nielsen, S. O. (1966) *Adv. Protein. Chem. 21*, 287–386.

Jelkmann, W., & Bauer, C. (1976) *Anal. Biochem. 75*, 382–388.
Karplus, M., & McCammon, J. A. (1981) *CRC Crit. Rev. Biochem. 9*, 293–349.
Kawamura-Konishi, Y., & Suzuki, H. (1988) *Biochem. Biophys. Res. Commun. 156*, 348–354.
Kuriyan, J., Wilz, S., Karplus, M., & Petsko, G. A. (1986) *J. Mol. Biol. 192*, 133–154.
Lakowicz, J. R., & Weber, G. (1973) *Biochemistry 12*, 4171–4179.
Li, X. Y., & Spiro, T. G. (1988) *J. Am. Chem. Soc. 110*, 6024–6033.
Linderstrom-Lang, K. (1955) *Spec. Publ.—Chem. Soc. 2*, 1–24.
Makinen, M. W., Houtchens, R. A. & Caughey, W. S. (1979) *Proc. Natl. Acad. Sci. U.S.A. 76*, 6042–6046.
Massat, A. (1987) Ph.D. Thesis, Université Paris VII.
McCammon, J. A., Gelin, B. R., & Karplus, M. (1977) *Nature 267*, 585–590.
Moffat, K., Deatherage, J. F., & Seybert, D. W. (1979) *Science 206*, 1035–1042.
Morgan, B., & Dolphin, D. (1987) *Struct. Bonding 64*, 115–204.
Norvell, J. C., Nunes, A. C. & Schoenborn, B. P. (1975) *Science 190*, 568–570.
Ormos, P., Braunstein, D., Frauenfelder, H., Hong, M. K., Lin, S. L., Sauke, T. B., & Young, R. D. (1988) *Proc. Natl. Acad. Sci. U.S.A. 85*, 8492–8496.
Oyanagi, H., Iizuka, T., Matsushita, T., Saigo, S., Makino, R., & Ishimura, Y. (1986) *J. Phys. 47*, C8-1147–C8-1150.
Padlan, E. A., & Love W. E. (1975) *J. Biol. Chem. 249*, 4067–4078.
Peng, S. M., & Ibers, J. A. (1976) *J. Am. Chem. Soc 98*, 8032–8036.
Perutz, M. F. (1968) *J. Cryst. Growth 2*, 54–56.
Perutz, M. F. (1970) *Nature 228*, 726–739.
Perutz, M. F. (1989) *Trends Biochem. Sci. 14*, 42–44.
Phillips, S. E. V. (1978) *Nature 273*, 247–248.
Phillips, S. E. V. (1980) *J. Mol. Biol. 142*, 531–554.
Phillips, S. E. V., & Schoenborn, B. P. (1981) *Nature 292*, 81–82.
Pin. S., Alpert, B., & Michalowicz, A. (1982) *FEBS Lett. 147*, 106–110.
Pin. S., Valat, P., Cortes, R., Michalowicz, A., & Alpert. B. (1985) *Biophys. J. 48*, 997–1001.
Potter, W. T., Hazzard, J. H., Kawanishi, S., & Caughey, W. S. (1983) *Biochem. Biophys. Res. Commun. 116*, 719–725.
Potter, W. T., Houtchens, R. A. & Caughey, W. S. (1985) *J. Am. Chem. Soc. 107*, 3350–3352.
Potter, W. T., Hazzard, J. H., Choc, M. G., Tucker, M. P., & Caughey, W. S. (1990) *Biochemistry 29*, 6283–6295.
Rholam, M., Scarlata, S., & Weber, G. (1984) *Biochemistry 23*, 6793–6796.
Royer, C. A. & Alpert, B. (1987) *Chem. Phys. Lett. 134*, 454–460.
Satterlee, J. D., Teintze, M., & Richards, J. H. (1978) *Biochemistry 17*, 1456–1462.
Shaanan, B. (1982) *Nature 296*, 683–684.
Shaanan, B. (1983) *J. Mol. Biol. 171*, 31–59.
Singh, G. P., Parak, F., Hunklinger, S., & Dransfeld, K. (1981) *Phys. Rev. Lett. 47*, 685–688.
Somogyi, B., Matko, J., Papp, S., Hevessy, J., Welch, G. R. & Damjanovich, S. (1984) *Biochemistry 23*, 3403–3411.
Sugita, Y., Nagai, M., & Yoneyama, Y (1971) *J. Biol. Chem. 246*, 383–388.
Traylor, T. G., & Berzinis A. P. (1980) *Proc. Natl Acad. Sci. U.S.A. 77*, 3171–3175.
Traylor, T. G., Mitchell, M. J., Tsuchiya, S., Campbell, D., Stynes, D. V., & Koca, N. (1981) *J. Am. Chem. Soc. 103*, 5234–5236.
Urban, S., Horak, M., & Vitek, A. (1976) *Collect. Czech. Chem. Commun. 41*, 3685–3690.
Ward, B., Wang, C. B., & Chang, C. K. (1981) *J. Am. Chem. Soc. 103*, 5236–5238.
Yu, N. T., Kerr, E. A., Ward, B., & Chang, C. K. (1983) *Biochemistry 22*, 4534–4540.
Zerner, M., Gouterman, M., & Kobayashi, H. (1966) *Theor. Chim. Acta 6*, 363–400.